

On the Cold Forging of 6082 H13 and T4 Aluminum Alloy Bushes

¹Buğra Karahan, ¹Umut İnce, ¹Sezgin Yurtdaş, ¹N. Emrah Kılınçdemir, ²Fuat Can Ağarer, *¹Cenk Kılıçaslan
¹Norm Cıvata San. ve Tic. A.Ş., A.O.S.B., İzmir, Turkey
²Norm Somun San. ve Tic. A.Ş., A.O.S.B., İzmir, Turkey

Abstract:

In this study, manufacturability of Ø23x36 aluminum bushes with EN AW 6082-AlSi1MgMn aluminum alloy was investigated. Two different pretreated EN AW 6082 alloys, H13 (strain-hardened) and T4 (solution annealing and naturally aged) were used in the present study and cold forging performance of the alloys was evaluated comparatively. Compression tests were carried out at different temperatures and strain rates to model the flow stress of the alloys. Extrusion tests were carried out on Zwick test machine in order to determine the material flow and sticking behavior. Cold forging trials were performed on a press having 300 tones capacity in Norm Fasteners. All experiments and forging operation were also coupled with finite element (FE) simulations by using Simufact.forming commercial software. Extrusions tests showed that the level of sticking phenomenon on dies are high for T4 alloy in contrast to H13 alloy. Cold forging trial showed that both alloys can be forged into desired shape without experiencing any failure. It was seen that surface roughness parameter of the cold forged T4 and H13 bushes was 3.81 µm and 0.99 µm, respectively. Numerical and experimental compression force-displacement curves were also found to be in good agreement.

Key words: Aluminum, EN AW 6082, cold forging, simulation.

1. Introduction

Cold forging is an extremely important and economical way for designers to create automotive components with high production rates and good mechanical strength. As a result of the developments in forging technology, complex parts such as non-standard bolts and nuts, ball joints and gears can be formed with better mechanical properties and geometrical accuracy [1-2]. Some of the advantages provided by this process include: (a) high production rates, (b) excellent dimensional tolerances and surface quality of forged parts, (c) significant savings in material in contrast to machining, (d) high tensile strength at the forged part, (e) suitable grain flow for higher strength [3].

In modern transportation sector, using the lightweight components is necessary due to economic and environmental restrictions. In the last decade, emission reduction ratios have been determined

*Corresponding author: Address: Norm Cıvata San. ve Tic. A.Ş., A.O.S.B., 35620, İzmir TURKEY. E-mail address: cenk.kilicaslan@norm-fasteners.com.tr, Phone: +902323767610

by governments. This ratio is aimed to be reduced to 95 g CO₂ / km with a 27% reduction by 2020 under the EU Regulation No 443/2009 [4]. In addition, lightweight structures used in the automotive industry are important for enhancing safety and driving comfort [5]. Weight reduction strategies are classified into four main categories as: material lightweight design, component lightweight design, functional lightweight design and conditional lightweight design [6].

The reduction in vehicle weight is mainly related to the use of lightweight materials such as aluminum alloys [7-8]. Aluminum alloys exhibit an attractive combination not only for a long service life but also low density, high specific strength, formability and excellent corrosion resistance, but also an important requirement for recycling [9-10]). 6xxx alloys within this group have been extensively studied due to technical considerations and reliable strength can be obtained by precipitation hardening. 6xxx series are also widely used for automotive and aerospace components due to their impact on weight reduction [11]. The 6082 alloy in this group is predominant due to its combination of higher mechanical properties, excellent corrosion resistance, convenience for T6 aging, and good weldability when compared to 6xxx alloys [12-13].

Although aluminum alloys exhibit nearly equivalent stiffness and two times higher specific strength compared to steel, they are disadvantageous in terms of raw material cost. Therefore, it is necessary to reduce the waste material and reduce the number of defective parts by using process optimization due to high raw material cost of aluminum [14]. Anjabin and Taheri [15] investigated the effect of different aging parameters on the mechanical properties of the 6082 alloy in their work. Flow curves were determined with uni-axial tensile tests at room temperature and material model was constituted. In addition, the force-displacement curves were analyzed and the experimental data and the model were compared. To verify the results which were predicted by the model, uni-axial compression was conducted using Abaqus software. Experiment and simulation results showed that the flow behavior of 6082 alloy is divided into two groups for underage condition and overage condition. According to this, flow stress increased and the uniform elongation decreased with increasing the aging temperature or aging time in underage condition. In contrast, increase in aging time and temperature leads to decrease in flow stress and increase in uniform elongation. Wang et al. [16] investigated the hot deformation behavior of 6082 alloy. True stress-true strain curves are obtained by performing compression tests at different temperatures (425 °C, 450 °C, 475 °C, 500 °C) and strain rates (0.01 s⁻¹, 0.1 s⁻¹, 1 s⁻¹, 10 s⁻¹). According to results, flow stress was found to increase with increasing strain rate and decreasing deformation temperature. The optimum hot working condition for 6082 aluminum alloy at the strain of 0.4 was found to be 470-490 °C and 0.1-0.3 s⁻¹ as strain rate. Ishikawa et al. [14] investigated the effects of thermal pulls on cold forged aluminum parts. As a result of the high thermal conductivity of aluminum compared to other metals, the thermal geometry changes in aluminum alloys have been pointed out. In the study, FE analysis was carried out using Simufact.forming software. These analyzes have shown that non-uniform temperature distributions cause local heat shrinkage on the part. Cylindrical compression tests were carried out to simulate flow curves of EN AW 6061 alloy and simulations have been conducted. Bay et al. [17] calculated friction stress for aluminum 6082 alloy, steel, and stainless steel by adopting a tribology testing system that can be simulated at different pressures, reduction ratios, surface propagation, sliding dies, and die-to-work interface temperatures. FE and

laboratory test results were analyzed and evaluated together. The results showed that the pressure and interface temperature between the die-workpiece were significantly more effective than other factors. Dubar et al. [18] investigated the effect of MoS₂ lubricant on sticking behavior of aluminum 6082 alloy during cold forging. In this study, FE simulations and experimental studies were evaluated comparatively. According to results, MoS₂ lubricant reduced the value of friction coefficient from 0.5-0.7 to 0.006-0.15. Sanjari et al. [12] used FE to calculate the stress field in the radial forging process of the 6082 alloy at different operating conditions and compare with the experimental results obtained by the micro hardness test. In addition, the effects of various process parameters such as friction, die angle, axial feed, back push and front pull forces on the strain field were investigated. Findings have shown that the heterogeneity of deformation decreases with increase in die angle and decrease in back push and friction.

Although there have been many studies corresponding to forming or determining mechanical properties of aluminum alloys in the literature, no study has been conducted on the manufacturability of aluminum bushes with EN AW 6082. In addition to the effect of pretreatment conditions of EN AW 6082 on final product surface quality is unknown. In order to fill this gap in the literature, EN AW 6082 alloy is considered on the basis of pretreated conditions H13 (strain-hardened) and T4 (solution annealing and naturally aged). The effect of H13 and T4 on the final product surface quality was investigated by experimental and computer aided engineering studies.

2. Materials and experimental procedure

2.1. Materials

In this study, Ø24 EN AW 6082 (AlSi1MgMn) alloy supplied by Drahtwerk ELISENTAL GmbH and chemical composition is given in Table 1. The alloy was produced in the form of wire rod by continuous casting and was prepared as pretreated H13 and T4. Specimens were prepared by machining to be used in compression and extrusion tests.

Table 1. Chemical composition of the EN AW 6082 alloy used in the present study.

Si	Fe	Cu	Mn	Mg	Zn	Ti	Al
0.7-1.30	<0.50	<0.10	0.40-1.0	0.60-1.20	<0.20	<0.10	Balance

2.2. Experimental procedure

Compressive tests have been carried out to determine the flow curves of EN AW 6082 alloy at different temperatures and different strain rates. Cylindrical samples with a diameter of 8 mm and a length of 12 mm were prepared in accordance to ASTM E9-89 standard for compression tests and Zwick / Roell Z600 universal tester was used in the tests. Compression tests were carried out at nominal strain rates of 0.001, 0.1 s⁻¹ and at temperatures of 20, 100 and 200 °C. The force-displacement curves were transformed into stress-strain curves firstly and then true stress-true plastic strain curves were drawn. Finally, the data is defined to Simufact.forming commercial FE

software. The simulations of the compression tests were carried out at different temperatures and different strain rates to verify the models and compared with the experimental data. In addition to the strain rates used in the tests, the simulations were repeated at the average forging machine strain rate (approx. 50 s^{-1}). The simulation model of the compression test is shown in Figure 1.

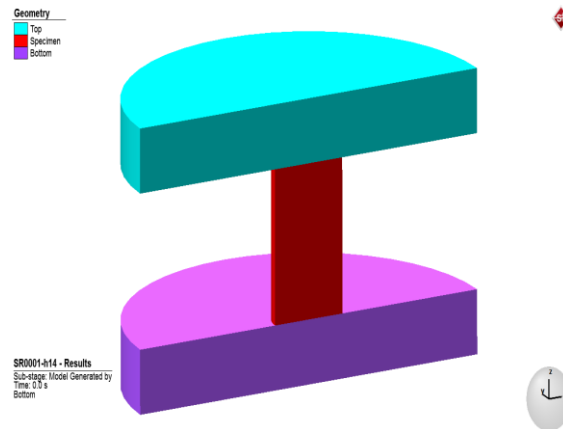


Figure 1. Compression simulation model.

Test and simulation studies were carried out to determine the behavior of EN AW 6082 alloy during extrusion. Samples with a diameter of 21.65 mm and a length of 40 mm were prepared for the extrusion tests and Zwick / Roell Z400 mechanical tester was used. In addition, the sticking phenomenon during the process was investigated. The technical drawing of the WC-Co die used in the extrusion tests is given in Figure 2. The extrusion ratio of in this die is 0.494 (49.4%) and hydraulic forging grease was used as lubricant.

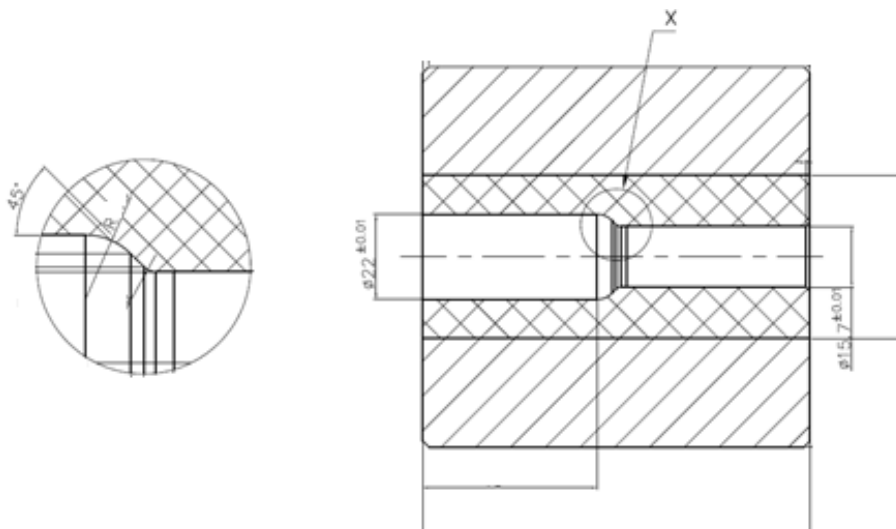


Figure 2. Technical drawing of the extrusion die.

After identifying the flow stress curves and sticking behavior of the EN AW 6082 alloy with material conditions H13 and T4, cold forging station design was modeled in the Simufact.forming FE software and the prototype production was performed. In these experiments Hyodong HNP 627 cold forging machine with a capacity of 300 tons was used. In the study, Zeiss Stemi 508 stereo-zoom microscope was used for macroscopic examinations and surface roughness analyzes were performed on Ambios Technology XP-2 high-resolution surface profilometer.

3. Results and discussions

The engineering stress-strain curves of the EN AW 6082-H13 and EN AW 6082-T4 are given in Figures 3 (a) and 3 (b), respectively. It was found that EN AW 6082-H13 showed lower stress values and the yield stress of the H13 decreased with increasing temperatures. Although the stress values of EN AW 6082-T4 decrease due to increase in temperature, it is not as high as H13. In particular, no significant decrease in the yield stress of T4 was observed. In addition to these results, an increase in the stress values of H13 was observed with an increase of the quasi-static strain rate by about 100 times at room temperature. However, the increase in strain rates caused an adverse effect in T4 and decrease in stress value was occurred. The yield stress of H13 was found to be 140 MPa at room temperature, 130.6 MPa at 100 °C and about 107 MPa at 200 °C. The yield stress value of T4 was determined to be 130 MPa.

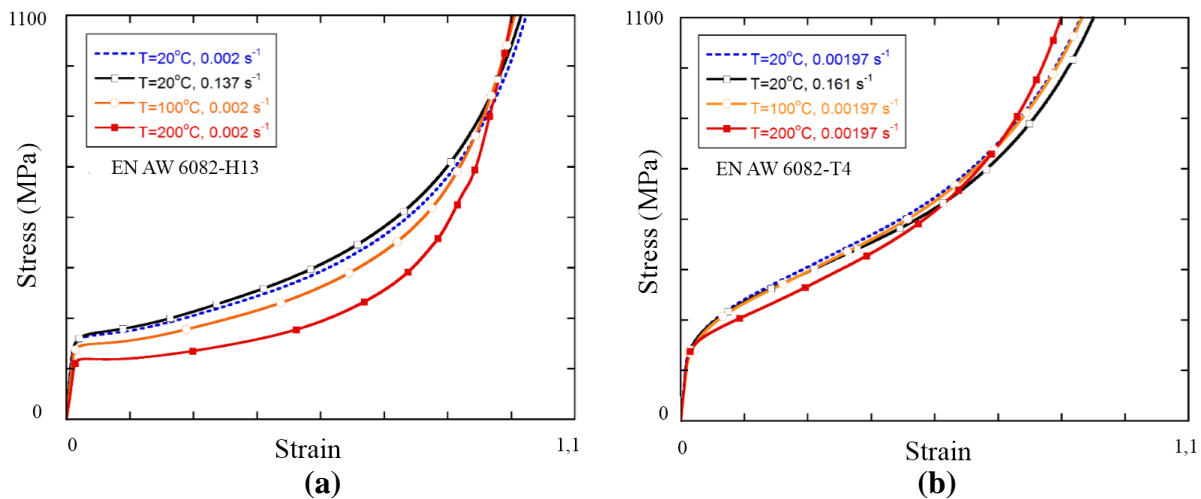


Figure 3. Stress-strain curves of EN AW 6082 alloy; (a) H13, (b) T4.

The comparison of the experimental results with the simulations of EN AW 6082-H13 and EN AW 6082-T4 at different strain rates at room temperature is given in Figure 4. Simulations and experiment results are in quite good agreement. It has been found that the temperature in the sample rises to 150 °C at high strain rate (50 s^{-1}). This temperature increase in the sample caused a decrease in the force values for EN AW 6082-H13 due to increase in temperature is more dominant than the increase in strain rate. However, there is no significant change in force values for T4 despite the increase in temperature and strain rate.

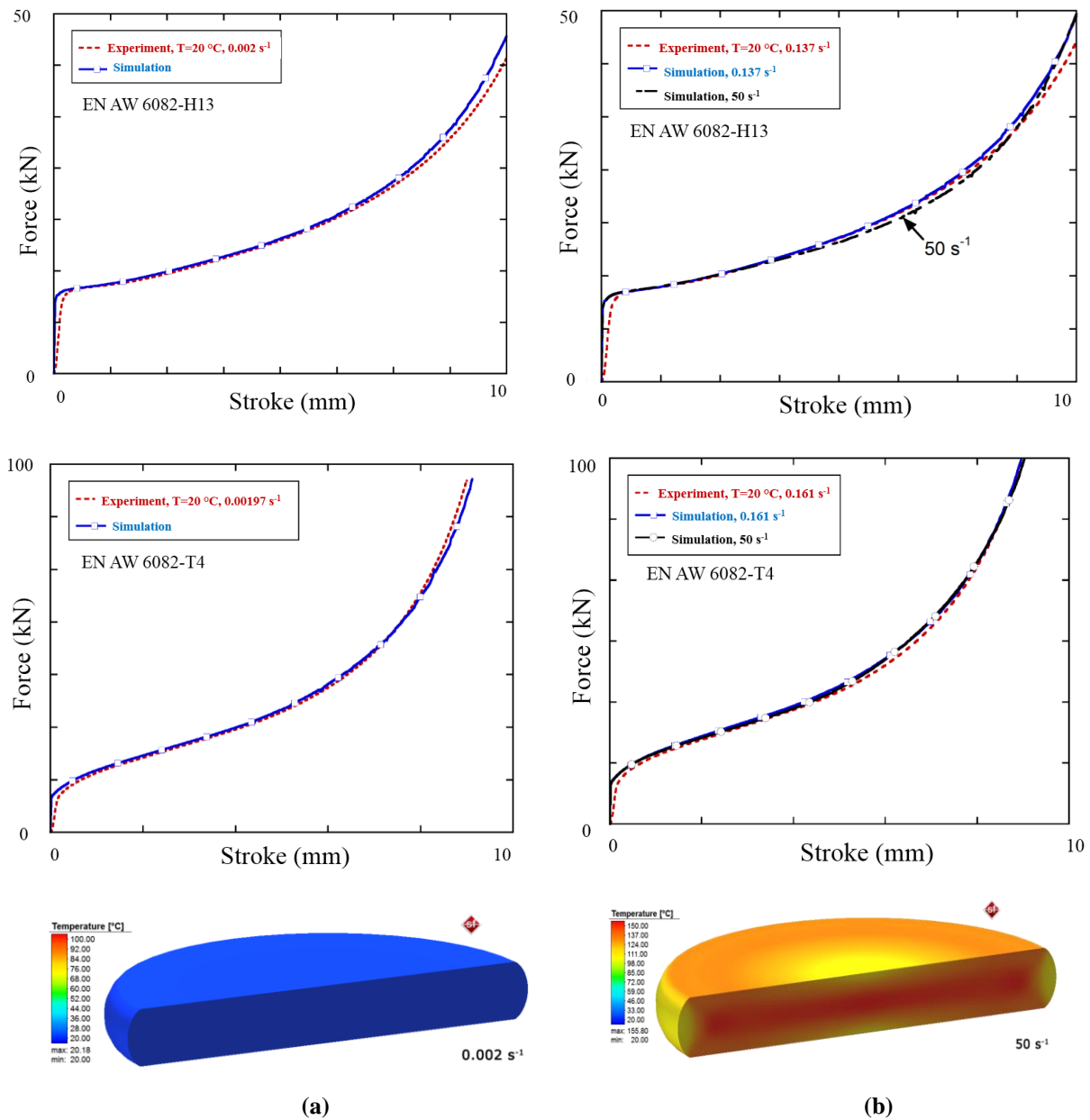


Figure 4. Simulation results and temperatures in the samples for EN AW 6082-H13 and T4; (T=20 °C)
 (a) $\dot{\epsilon} = 0.002 \text{ s}^{-1}$ (b) $\dot{\epsilon} = 0.137 \text{ s}^{-1} - 50 \text{ s}^{-1}$.

Figure 5 shows the surface condition on the samples after extrusion. Defects in the form of ripples were identified on the extrusion surfaces for pretreated H13 and T4. After the tests it was seen that the material chips were accumulated in the shoulder region of the extrusion die. Therefore, surface defects are estimated to be due to sticking phenomenon. On specimens of H13, surface defects begin at the shoulder region and condense at the shaft, however the defects is found to be distributed over the entire surface and more intense on T4 specimens. These findings are consistent with effective plastic strain values.

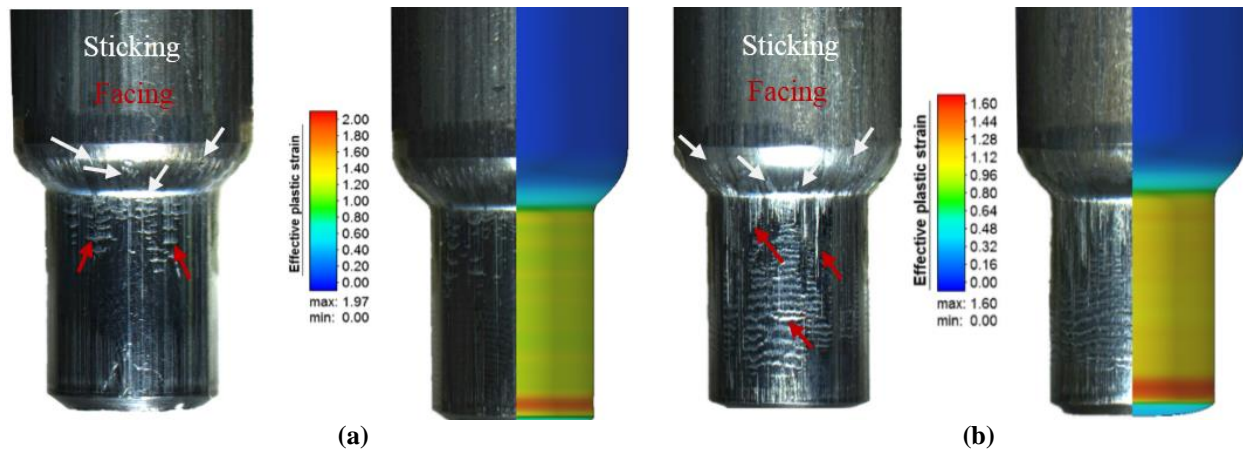


Figure 5. Material surface condition after extrusion and effective plastic strain distributions; (a) EN AW 6082-H13 (b) EN AW 6082-T4

At the last stage of the work, aluminum bushes production trials were carried out. Figure 6 shows the cold forging station design and station samples. Bushes are manufactured by deforming the workpiece in consecutive forging stations. Therefore, each station has a different design and a different forming steps take place. The aluminum bushes were successfully manufactured with the EN AW 6082 alloy with both H13 and T4 conditions without experiencing any forming failure or fracture.

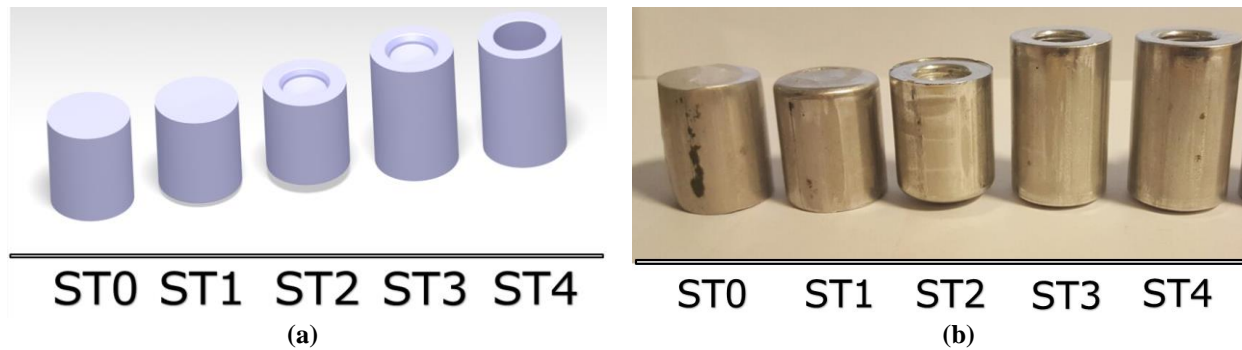


Figure 6. Aluminum bushes a) station design (b) station samples.

The prototypes were examined macroscopically and surface condition of the EN AW 6082-H13 and EN AW 6082-T4 were compared. According to Figure 7, it is observed that the final product surface qualities are different from each other and it was found that the amount of facing on the surface of bushes produced with EN AW 6082-T4 alloy is higher than EN AW 6082-H13.

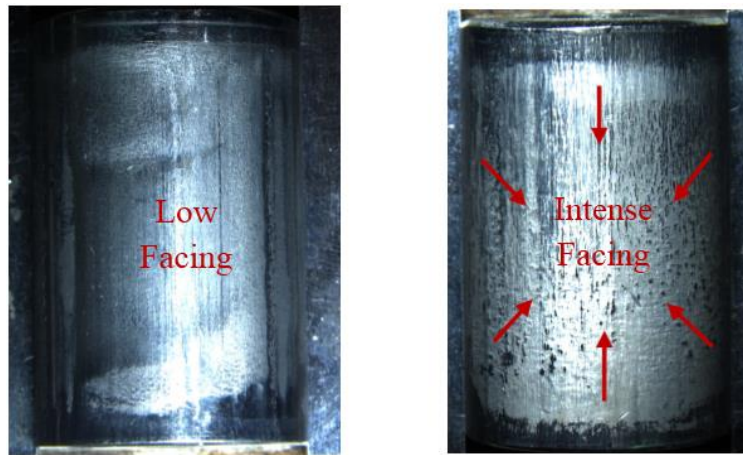


Figure 7. Macroscopic examination of bushes produced with EN AW 6082 (a) H13 (b) T4.

In addition, the roughness parameters are comparatively measured so that the surface qualities of the aluminum bushes produced with EN AW 6082-H13 and EN AW 6082-T4 can be analytically evaluated. The values are given in Table 2 and the corresponding curves are given in Figure 8. When comparing the surface roughness parameters for H13 and T4, values are compatible with extrusion test results and macroscopic examinations. The R_a value for T4 is about 3-4 times greater than H13 and was measured as $3.81 \mu\text{m}$.

Table 2. Surface roughness parameters of bushes produced with EN AW 6082-H13 and T4.

Pretreated Conditions	Surface Roughness Parameters (μm)			
	R_a	R_q	R_t	R_z
H13	0.99	1.26	8.99	6.80
T4	3.81	4.73	31.59	21.46

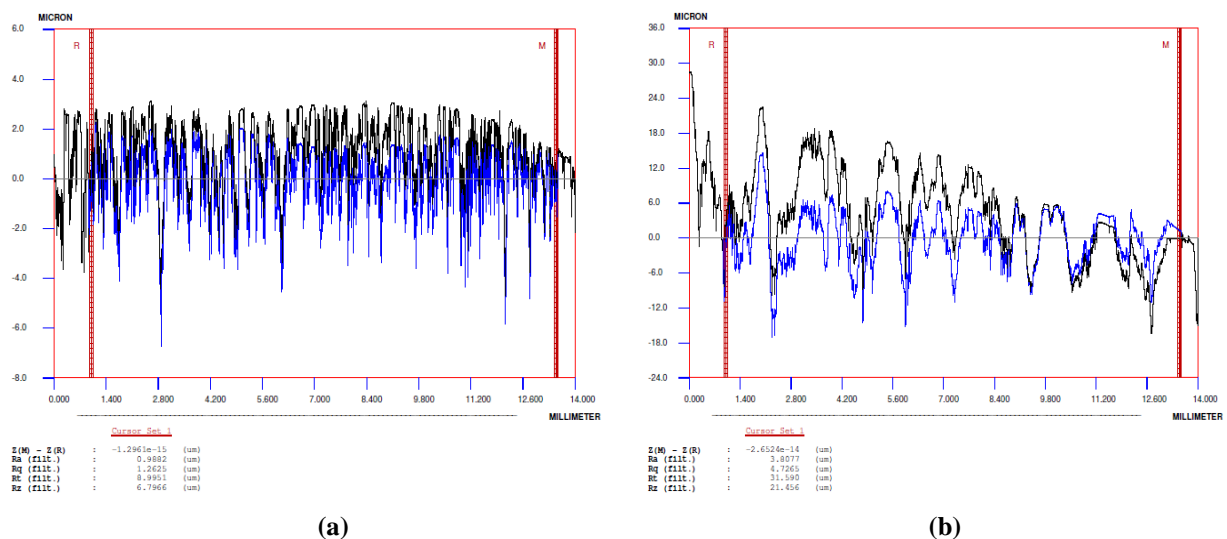


Figure 8. Surface roughness curves of bushes produced with EN AW 6082 (a) H13 (b) T4.

Conclusions

In this study, the manufacturability of Ø23x36 aluminum bushes with pretreated EN AW 6082 (H13 and T4) was investigated. Flow stress curves were determined by compressive tests. Also, material flow and sticking behavior were determined by extrusion tests and roughness parameters were obtained with high resolution surface profilometer. The obtained results were compared with the FE analysis and confirmed.

According to results:

- EN AW 6082-H13 has a higher sensitivity to temperature than T4. Compression test results at different temperatures showed that, the yield stress of H13 was found to change between 140 MPa and 107 MPa. No significant change was observed in T4.
- Stress value of H13 increased with increasing strain rate. However, a decrease in T4 was observed.
- Compression simulations were carried out at the strain rates observed in cold forging machines (50 s^{-1}) and the temperature in the sample reached $150 \text{ }^\circ\text{C}$. It was determined that the softening observed due to the temperature increase was more dominant than strain hardening due to the high strain rate for H13 and the decrease in the force values was found. However, no significant change was observed for T4.
- The surface defects is found to be distributed over the entire surface and more intense on T4 specimens after extrusion tests.
- Ø23x36 aluminum bushes was produced successfully in production trials with both H13 and T4.
- It was calculated that R_a parameter of the cold forged H13 and T4 bushes as $0.99 \text{ } \mu\text{m}$ and $3.81 \text{ } \mu\text{m}$, respectively.

Acknowledgments

The authors thanks to employees of NORM CIVATA Co. and NORM SOMUN Co.

References

- [1]Jensrud O, Pedersen K. Cold forging of high strength aluminum alloys and the development of new thermomechanical processing, *J Mater Process Technol* 1998; 80–81:156–60.
- [2]Birol Y, Ilgaz O, Akdi S, Unuvar E. Comparison of cast and extruded stock for the forging of AA6082 alloy suspension parts, *Adv. Mater. Res.* 2014; 939: 299–304.
- [3]Oh SI, Wu WT, Tang JP. Simulations of cold forging processes by the deform system, *Journal of Materials Processing Technology* 1992; 35: 357-370
- [4]European Union. Regulation (EC) No 443/2009 of the European Parliament and of the Council setting emission performance standards for new passenger cars as part of the Community's integrated approach to reduce CO₂ emissions from light-duty vehicles, 2009.

- [5] Kleiner M, Geiger M, Klaus A. Manufacturing of Lightweight Components by Metal Forming, *CIRP Annals - Manufacturing Technology* 2003; vol. 52, pp. 521-542.
- [6] Tekkaya AE, Khalifa NB, Grzanic G, Hölker R. Forming of lightweight metal components: Need for new technologies, *Procedia Engineering* 2014; 81: 28 – 37.
- [7] Davies G. *Materials for automotive bodies*. 2nd ed., 2012.
- [8] Jeswiet J, Geiger M, Engel U, Kleiner M, Schikorra M, Duflou J. Metal forming progress since 2000, *CIRP J Manuf Sci Technol* 2000; 1: 2–17.
- [9] Davis JR. *Aluminum and Aluminum Alloys*. ASM Specialty Handbook, ASM International, Materials Park, OH, 1996.
- [10] Kuhlman GW. Forging of Aluminum Alloys, vol.14, *ASM Handbook*, 9th ed., ASM Int.1988, pp. 244–254.
- [11] Bouquerel J, Diawara B, Dubois A, Dubar M, Vogt JB, Najjar D. Investigations of the microstructural response to a cold forging process, *Materials and Design* 2015; 68: 245–258.
- [12] Geoffroy N, Vittecoq E, Birr A, de Mestral F, Martin J-M. Fatigue behaviour of an arc welded Al–Si–Mg alloy. *Scr Mater* 2007; 57: 349–52.
- [13] Tveiten B, Fjeldstad A, Harkegard G, Myhr O, Bjorneklett B. Fatigue life enhancement of aluminium joints through mechanical and thermal prestressing, *Int J Fatigue* 2006; 28: 1667–76.
- [14] Ishikawa T, Ishiguro T, Yukawa N, Goto T. Control of thermal contraction of aluminum alloy for precision cold forging, *CIRP Annals - Manufacturing Technology* 2014; 63: 289–292.
- [15] Anjabin N, Taheri AK. The effect of aging treatment on mechanical properties of AA 6082 alloy: modeling and experiment, *Iranian Journal of Materials Science & Engineering*, 2010, Vol. 7, N.2.
- [16] Wang P, Jiang H, Zhang R, Huang S. Study of Hot Deformation Behavior of 6082 Aluminum Alloy, *Materials Science Forum* 2016; 877: 340-346.
- [17] Bay N, Eriksen M, Tan X, Wibom O. A friction model for cold forging of aluminum, steel and stainless steel provided with conversion coating and solid film lubricant, *CIRP Annals - Manufacturing Technology* 2011; 60: 303–306.
- [18] Dubar L, Pruncu CI, Dubois A, Dubar M. Effects of contact pressure, plastic strain and sliding velocity on sticking in cold forging of aluminium billet, *Procedia Engineering* 2014; 81: 1842 – 1847.
- [19] Sanjari M, Saidi P, Taheri AK, Zadeh MH. Determination of strain field and heterogeneity in radial forging of tube using finite element method and microhardness test, *Materials and Design* 2012; 38: 147–153.